Ultrasound Current Source Density Imaging of a Time-varying Current Field in a Multielectrode Nerve Chamber

Ragnar Olafsson, Qian Li, Zhaohui Wang, Pier Ingram, and Russell S. Witte
Department of Radiology, University of Arizona
Tucson, Arizona, USA
rolafsso@email.arizona.edu

***Abstract*— Drug resistant epilepsy can in some cases be treated with surgery. To minimize potentially crippling side effects of surgery, a detailed functional map of the brain is usually required prior to resection. Conventional mapping techniques rely on a coarse grid of electrodes with limited spatial resolution. Ultrasound Current Source Density Imaging (UCSDI) is new high resolution method to image electric current based on ultrasound. UCSDI potentially enhances conventional mapping procedures as it produces 4D (space and time) maps of current flow co-registered to ultrasound. In this paper, we describe a new system for studying UCSDI in peripheral nerves and neural tissue. This system allows multi-electrode detection of conventional electrophysiological signals simultaneous with UCSDI. UCSDI was used to map short bursts of current injected through the rat sciatic nerve. The amplitude of the current was varied to test the sensitivity of the system. The detection threshold was 0.1 mA/cm^2 at ~250 kPa, well within range for detecting bioelectric signals in neural tissue.**

Keywords; acoustoelectric, UCSDI, epilepsy, bioelectromagnetism, neuroelectrophysiology, electrical brain mapping

I. Introduction

Approximately 1% of the general population and 3 million U.S. citizens suffer from epilepsy. In the most severe cases, over 20% do not respond adequately to anti-seizure medication and become candidates for surgical removal of the portion of the brain causing the seizure. A detailed functional map of the brain is crucial to localize the epileptic focus and identify brain areas needed for survival (e.g., sensory and motor). Damage to these critical areas could lead to slurred speech or paralysis, for example. Existing electrical mapping techniques are laborious and imprecise due to limitations with conventional electrophysiological methods; one limitation is due to the tradeoff between spatial resolution and degree of invasiveness. Minimally invasive surface electrode arrays detect average activity of a large population of cells, whereas sharp penetrating electrodes are capable of tracking individual neurons. We have developed over the last few years Ultrasound Current Source Density Imaging (UCSDI), a new method for mapping electric current that potentially enhances existing approaches to identify an epileptic focus and map critical brain areas. The potential advantages of UCSDI are 1) improved spatial resolution determined by the ultrasound beam, 2) multidimensional mapping with enhanced penetration using as few as two recording electrodes, and 3) automatic registration with pulse echo ultrasound for depicting brain structure. We have previously demonstrated UCSDI in a variety of preparations, including mapping of the cardiac activation wave in the live rabbit heart [1-8]. As an important step towards mapping electric brain signals using ultrasound, this study describes UCSDI in a well-controlled nerve chamber for mapping fast time-varying current flow.

We gratefully acknowledge the support of the NIH R01 EB009353 Advanced Research Institute for Biomedical Imaging (ARIBI), Technology Research Infrastructure Fund (TRIF), and Department of Radiology at the University of Arizona.

II. Ultrasound Current Source Density Imaging

UCSDI is based on the acoustoelectric (AE) effect, an interaction between ultrasound and electrical resistivity. In its simplest form, the AE effect can be described by

$$\frac{\Delta\rho}{\rho_0} = -K_I \Delta P, \qquad (1)$$

where $\Delta\rho$ is the change in resistivity, ρ_0 the dc resistivity, ΔP the acoustic pressure and K_I an interaction constant whose value is 10^{-9} Pa^{-1} in a 0.9% NaCl solution [9-11]. When focused ultrasound transducers are used, the resistivity of the focal region is selectively modulated at the ultrasound frequency. If

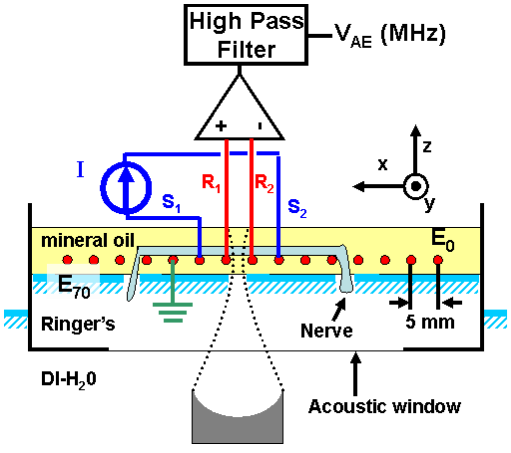

Figure 1. Experimental setup. The rat sciatic nerve was placed on a linear array of stainless steel electrodes (red dots named E_i, i=0,5,…70) and immersed in mineral oil for electric insulation and acoustic coupling. AE signals were recorded from a single pair of electrodes (R_1,R_2), while current was injected through adjacent electrodes (S_1, S_2).

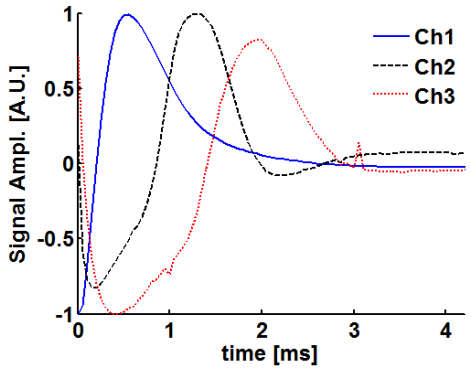

Figure 2. Low frequency bioelectric signals acquired from a rat sciatic nerve. The nerve was stimulated between electrodes E_{15} and E_{10} with a rectangular pulse (10 V, 830 µs) and signals were recorded on three pairs of electrodes Ch1 (E_{30}-E_{25}), Ch2 (E_{40}-E_{35}), and Ch3 (E_{50}-E_{45}). The signals are offset in time because the compound action potential propagated along the nerve.

current flows through the focal region, by Ohm's law, an ultrasound modulated AE voltage signal can be measured with electrodes distant to the focal region. Just as with pulse echo ultrasound imaging, a UCSD image can be formed by collecting AE signals at different locations of the ultrasound beam with depth information determined by the speed of sound of the ultrasound pulse. A more complete mathematical description of UCSDI, including reconstruction of electrical sources and potentials, can be found in our recent publications [2, 5].

III. Methods

A. *Instrumentation*

The experimental geometry is shown in Fig. 1. A sciatic nerve was excised from a fresh rat cadaver immediately after euthanasia. The nerve was placed in mammalian Ringer's solution for maintenance (in mM: NaCl 118, KCl 5.9, $MgCl_2$ 1.2, Tris 5.0, Glucose 10, $CaCl_2$ 2.5, pH 7.4) in a multielectrode nerve chamber (NERVE2, BIOPAC Systems Inc., Goleta, CA). The nerve was placed on the electrodes and

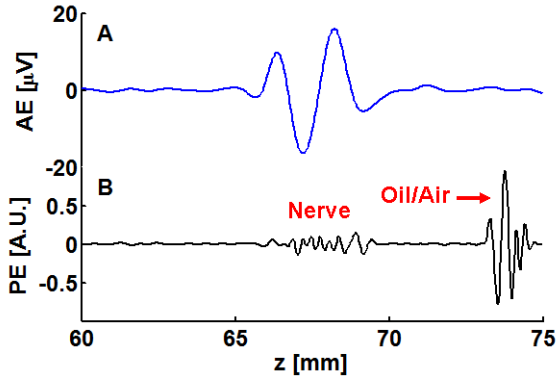

Figure 3. Sample radio frequency (RF) waveforms captured at y=0 and time = 17.8 msec. Plot B is the pulse echo (PE) trace showing both the nerve as well as the oil/air interface. Above it is plot A, the corresponding AE voltage trace captured simultaneously.

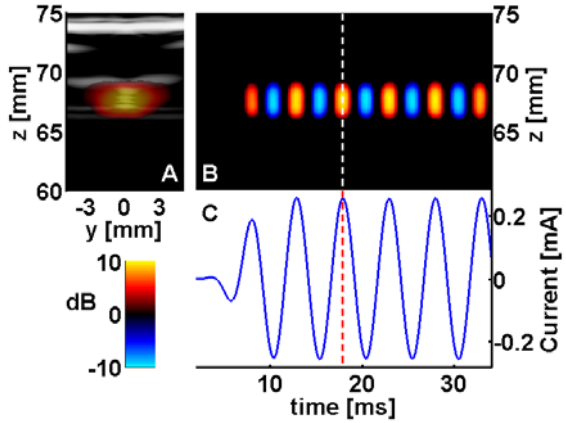

Figure 4. Ultrasound Current Source Density Images (UCSDI) of electric current burst in rat sciatic nerve. Image A is a B-mode short axis image of the nerve. The gray scale image is normal pulse-echo (PE) ultrasound with 30 dB dynamic range while the UCSDI image is overlayed in hot/cold colorscale. Image B is an M-mode UCSDI image that corresponds to the line y=0 in image A. Plot C is the low frequency current signal shown on the same time scale as image B. The time to which image A corresponds is indicated with a dashed lines in images B and C.

immersed in mineral oil for acoustic coupling and electrical insulation. Low frequency bioelectric signals were detected from the nerve; examples are depicted in Fig. 2. A single element transducer (2.25MHz, f/1.8, 69 mm focal length, V395, Panametrics, Waltham, MA) was focused on the nerve from below. A 10 cycle 200Hz current burst was injected by a signal generator (33220A, Agilent, Santa Clara, CA) through a pair of electrodes (S_1, S_2). The current was measured with a differential amplifier (DA1855A PR2, Lecroy, Chestnut Ridge, NY) as the voltage drop across a 1Ω resistor placed in series with the current injection electrodes. The current signal was sampled at 20kHz and digitized with a PCI card (6035E, National Instruments, Austin, TX). AE signals were captured from electrodes R_1 and R_2 and fed through an analog high pass filter (482 kHz, -3dB frequency) into a differential amplifier (1855, Lecroy) with a gain of 10 and 10 MHz bandwidth. The signal was further amplified 100 times (DA1855A PR2, Lecroy), low pass filtered at 5 MHz with an electronic filter (BLP-5+, Mini-Circuits, Brooklyn, NY), and sampled at 31.25 MHz by a fast acquisition board (PDA12, Signatec, Newport Beach, CA).

Experimental timing was provided by a field programmable gate array (FPGA) device (ezFPGA, Dallas Logic, Plano, TX). The FPGA sent out three timing signals: a pulse to trigger the PCI-6035E, a trigger delayed by 7 msec to the signal generator, and a burst of 170 triggers (205 µs trigger interval) to the ultrasound pulser/receiver (5077PR, Panametrics). The burst of ultrasound triggers was synchronized with the trigger to the PCI-6035E. The time delay ensured that data were also acquired just before the onset of the current burst for background noise measurement.

B. *Experimental Procedure*

Short axis AE and PE images were acquired by moving the transducer 10 mm (31 steps of 0.32 mm) along the y-axis. At

each position, current bursts were injected 128 times, and the resulting AE and PE signals were averaged. A short axis image was acquired at each of 10 different current amplitude settings between 0 mA and 0.5 mA peak to peak. As an additional control, the acquisition was repeated when the ultrasound was blocked by placing an air bubble below the acoustic window of the nerve chamber.

C. *Data Processing*

The AE data were converted to complex analytic form and band pass filtered in fast-time (0.3- 1.3 MHz, -3dB pass band) and slow time (160- 320 Hz, -3dB pass band). The short axis AE images were filtered laterally with a Gaussian spatial filter (FWHM = 1.2 mm). For comparison, the low frequency current waveform was filtered with the same slow time filter as the AE signals. Measurement sensitivity was estimated by plotting the AE signal to noise ratio (SNR) as a function of current density. The SNR was calculated from the rms value of the AE signal over a region of interest of 2.6 mm axial, 5 mm lateral, and 27 ms slow time with the noise estimated at 0 mA (signal generator output off). The dimensions of the window were based on the -6 dB envelope of the AE signal at the highest current setting.

IV. Results and Discussion

In this study we have demonstrated and characterized a new well controlled experimental system for imaging peripheral nerves and nerve tissue with UCSDI.

This system is based on a commercially available neural chamber with a simple geometry that can easily be modeled in software. The grid of electrodes allows simultaneous detection and tracking of conventional electrophysiological signals as Fig. 2 demonstrates. The simple geometry facilitates the interpretation of AE and PE signals as shown in Fig. 3. Notice that the frequency content of the AE signal is shifted down compared to the pulse echo. The AE signal is a spatio-temporal convolution between the acoustic pulse and the conductive area of the nerve. We suspect that that the nerve could act as a low pass filter in fast time because the electrical measurement is a spatial average over its cross section.

Representative images which correspond to the highest current setting (0.5 mA) are shown in Fig. 4. This figure shows

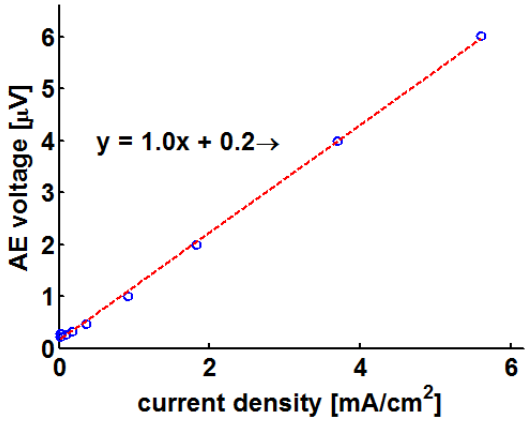

Figure 5. AE rms voltage as a function of current density

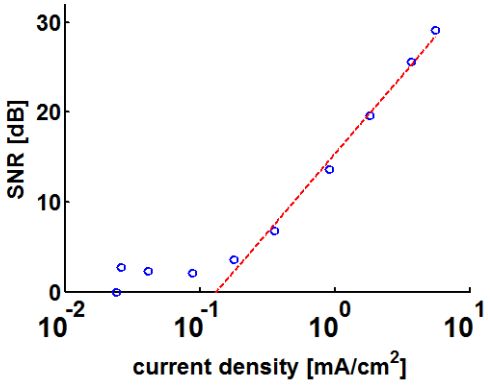

Figure 6. AE signal to noise ratio as a function of current density

that in this setup it is possible to resolve spatially and temporally electric current in a nerve with only two electrodes. Image 4A demonstrates that the UCSDI co-registers with the pulse-echo image while image 4B demonstrates that UCSDI image amplitude is proportional to the injected current waveform shown in image 4C. Figure 5 shows AE rms voltage as a function of current density. The current density was estimated assuming the nerve had a circular cross section 2 mm, determined from the pulse-echo signal. According to Ohm's law and the AE effect, the measured AE signal should be proportional to current density.

A plot of SNR versus current density is shown in Fig. 6. From this plot we can see that the trend line (red dashed line) intersects the noise floor between 0.1-0.2 mA/cm^2. The sensitivity is comparable to what we previously obtained in a rabbit heart and is much better than in our previous nerve setup [3, 7]. It is also smaller than the theoretical estimate of 0.5 mA/cm^2 for biological current [12].

These results show that we can potentially measure neural current signals with our current setup. But there is room for improvement. These results were obtained at a modest pressure level of 250 kPa. By increasing the acoustic pressure, sensitivity should improve accordingly.

V. Conclusions

We have demonstrated a new system for UCSDI imaging of neural tissue. The detection sensitivity at a modest acoustic pressure of 250 kPa is sufficient for detecting biological current.

This study is a steppingstone towards mapping bioelectric neural signals with UCSDI, which could potentially revolutionize pre-operative mapping in epileptic surgery by providing real time, high resolution 3D maps of the brain co-registered to pulse echo ultrasound.

Acknowledgment

We gratefully acknowledge the support of the NIH R01 EB009353, Advanced Research Institute for Biomedical Imaging (ARIBI), Technology Research Infrastructure Fund (TRIF), and Department of Radiology at the University of Arizona. We would also like to thank Michael Bernas for his assistance with the animal preparation.

REFERENCES

[1] R. Olafsson, R. S. Witte, C. Jia, S.-W. Huang, and M. O'Donnell, "Detection of Electrical Current in a Live Rabbit Heart using Ultrasound," in *2007 IEEE Ultrasonics Symposium*, New York, NY, 2007, pp. 989-992.

[2] R. Olafsson, R. S. Witte, S.-W. Huang, and M. O'Donnell, "Ultrasound Current Source Density Imaging," *IEEE Transactions on Biomedical Engineering,* vol. 55, pp. 1840-1848, July 2008.

[3] R. Olafsson, R. S. Witte, C. X. Jia, S. W. Huang, K. Kim, and M. O'Donnell, "Cardiac Activation Mapping Using Ultrasound Current Source Density Imaging (UCSDI)," *IEEE Transactions on Ultrasonics Ferroelectrics and Frequency Control,* vol. 56, pp. 565-574, Mar 2009.

[4] R. Olafsson, R. S. Witte, K. Kim, S. Ashkenazi, and M. O'Donnell, "Electric current mapping using the acousto-electric effect - art. no. 61470O," *Medical Imaging 2006: Ultrasonic Imaging and Signal Processing,* vol. 6147, pp. O1470-O1470, 2006.

[5] R. Olafsson, R. S. Witte, and M. O'Donnell, "Measurement of a 2D electric dipole field using the acousto-electric effect - art. no. 65130S," *Medical Imaging 2007: Ultrasonic Imaging and Signal Processing,* vol. 6513, pp. S5130-S5130, 2007.

[6] R. S. Witte, S., Olafsson, Ragnar and O'Donnell, Matthew, "Acousto-electric detection of current flow in a neural recording chamber," in *2006 IEEE International Ultrasonics Symposium*, Vancouver, BC, Canada, 2006, pp. 5-8.

[7] R. S. Witte, R. Olafsson, S. W. Huang, and M. O'Donnell, "Imaging current flow in lobster nerve cord using the acoustoelectric effect," *Applied Physics Letters,* vol. 90, pp. -, Apr 16 2007.

[8] R. S. Witte, T. Hall, R. Olafsson, S.-W. Huang, and M. O'Donnell, "Inexpensive acoustoelectric hydrophone for mapping high intensity ultrasonic fields," *Journal of Applied Physics,* vol. 104, p. 054701, 2008.

[9] J. Jossinet, B. Lavandier, and D. Cathignol, "The phenomenology of acousto-electric interaction signals in aqueous solutions of electrolytes," *Ultrasonics,* vol. 36, pp. 607-613, Feb 1998.

[10] J. Jossinet, B. Lavandier, and D. Cathignol, "Impedance modulation by pulsed ultrasound," *Electrical Bioimpedance Methods: Applications to Medicine and Biotechnology,* vol. 873, pp. 396-407, 1999.

[11] B. Lavandier, J. Jossinet, and D. Cathignol, "Experimental measurement of the acousto-electric interaction signal in saline solution," *Ultrasonics,* vol. 38, pp. 929-936, Sep 2000.

[12] J. Malmviou and R. Plonsey, "Chapter 8: Source-Field Models " in *Bioelectromagnetism: Principles and applications of bioelectric and biomagnetic fields* New York: Oxford University Press, 1995, pp. 148-158.